Ultrahigh Energy Storage in Multilayer Capacitors with Self-Assembled Glass-Like Matrix and Polar Clusters

Zhen Liu[*, #, a], *Minghao Liu*[#, a], *Tengfei Hu*[#, ad], *Xiang Niu*[bc], *Bin Zhou*[a], *Teng Lu*[*, b], *Cheng Yang*[b], *Fei Cao*[a], *Shengguo Lu*[*, c], *Yun Liu*[b], *Genshui Wang*[*, ad], *Junhao Chu*[e]

a. Key Laboratory of Inorganic Functional Materials and Devices, Shanghai Institute of Ceramics, Chinese Academy of Sciences, Shanghai 200050, China. E-mail: zhenliu@mail.sic.ac.cn, genshuiwang@mail.sic.ac.cn

b. Research School of Chemistry, The Australian National University, Canberrsa, ACT 2601, Australia. E-mail: teng.lu@anu.edu.au

c. School of Materials and Energy, Guangdong University of Technology, Guangzhou 510006, China. E-mail: sglu@gdut.edu.cn

d. School of Chemistry and Materials Science, Hangzhou Institute for Advanced Study, University of Chinese Academy of Sciences, Hangzhou 310024, China.

e. State Key Laboratory of Infrared Physics, Shanghai Institute of Technical Physics, Chinese Academy of Sciences, Shanghai 200083, China.

[#] These authors contributed equally to this work.

Electronic supplementary information (ESI) available. See DOI: …

Experimental Section

Bulk ceramic preparation: The $(Bi_{1/6}K_{1/6}La_{1/6}Na_{1/6}Sm_{1/6}Li_{1/6})TiO_3$ ceramics were prepared via traditional solid-phase reaction method. The high-purity powers of Li_2CO_3 (99.99%), Na_2CO_3 (99.8%), K_2CO_3 (99.9%), La_2O_3 (99.95%), Sm_2O_3 (99.99%), Bi_2O_3 (99.999%) and TiO_2 (99.9%) were weighted in the required stoichiometric ratios, then mixed with ethanol for 4 h using a ball mill. The dried mixture was calcined at 1150°C for 2 h, and the resulting product was ball milled again for 6 h using ethanol. After drying, the powers were mixed evenly with binder (7 *wt*.% PVA) and pressed into pellets with a diameter of 13 mm under 1.5 MPa. These pellets were calcined at 800°C for 2 h to

burn out PVA, and subsequently sintered at 1050 °C for 2 h to obtain bulk ceramics.

MLCC fabrication: The powder after the second ball milling was mixed with the dispersant (ammonium polyacrylate), binder (polyvinyl butyral), plasticizer (dioctyl pahthalate), and solvent (ethanol, ethyl acetate), then milled together for 24 h to obtain the tape-casting slurry. The slurry was subsequently prepared as tapes with a thickness ~ 6 μm using a tape caster, and the dried tapes were cut and printed with 70Ag/30Pd electrodes. Tapes with electrodes and blank tapes were stacked layer by layer according to the designed MLCC specifications and isostatically laminated as a bar block at 64 MPa. The bar block was then cut into individual blocks. Subsequently, they were heated at 270 °C for 2 h to remove organic binders, and then sintered at 1040°C for 2 h to obtain MLCCs.

Structure Characterization: The crystal structure of samples was ascertained by XRD, employing Bruker's D8 ADVANCE for in-situ assessments with Cu kalpha radiation. Raman spectroscopy was conducted using Renishaw's inVia reflex device. The micro-morphology of samples was examined using SEM, model S-4800 from Hitachi, Tokyo, Japan. Atomic scale structure analysis was performed using Spherical aberration-corrected STEM (JEM-ARM200F, JEOL Co. Ltd) equipped with a cold field-emission gun and a DCOR probe Cs-corrector (CEOS GmbH) operated at 200 kV. STEM images were acquired in annular dark-field (ADF) mode using a convergent semi-angle of 20.4 mrad and collection semi-angles ranging from 70 to 300 mrad. Subsequently, the positions of atomic columns are identified via 2D Gaussian fitting. Atomic PDF analysis based on synchrotron X-ray total scattering is conducted to reconstruct the 3D nanostructure and investigate the local structure. RMC refinement was performed on the RMC profile software. Both real-space (G(r) data) and reciprocal-space (S(Q)) are fitted during the refinement. A large supercell comprising 24 × 24 × 24 parent perovskite unit cells (69,120 atoms; ~94 × ~94 × ~94 $Å^3$) was constructed. In order to ensure structural and chemical plausibility, the bond valence sum (BVS), bond length and the coordination constraints were carefully considered for the RMC simulation. Different atoms occupying the same crystallographic positions were allowed to move and exchange during the simulation. Subsequently, the 3D polar displacements, polarization vectors, and stereographic projections were analyzed using MATLAB scripts based on the simulated supercell.

Property Measurement: For *P-E* loop measurements, bulk ceramics were ground to a thickness of ~ 50 μm and sputtered with Au electrodes with a diameter of 1 mm, and silver paste was used as

termination electrode for MLCCs. The *P-E* loop measurements were performed utilizing a ferroelectric testing device (aixACCT TF Analyzer 2000E). Dielectric characteristics were analyzed by a wide-temperature, wide-frequency dielectric spectrometer (Novocontrol GmbH, Concept 80). Charge-discharge (underdamped and overdamped) tests were performed on a commercial testing platform (CFD-001, Gogo Instruments Technology, Shanghai, China), which incorporated a tailored RLC (resistance, inductance, and capacitance) load circuit. The MLCCs employed in discharging test are consistent with those used in the *P-E* loop measurements.

Table S1. Comparison of the multiple cations introduced across different parameters.

Element	Bi	K	La	Na	Sm	Li
Valency	+3	+1	+3	+1	+3	+1
Ionic radius (Å, CN=12)	1.38	1.64	1.36	1.39	1.24	1.14
Atomic mass (u)	208.98	39.10	138.91	22.99	150.36	6.94
Electronegativity	2.02	0.82	1.10	0.93	1.17	0.98

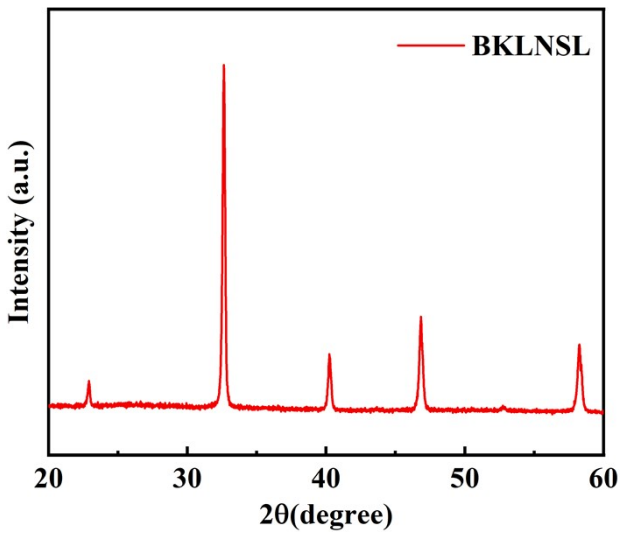

Figure S1. XRD pattern of the BKLNSL ceramics at room temperature.

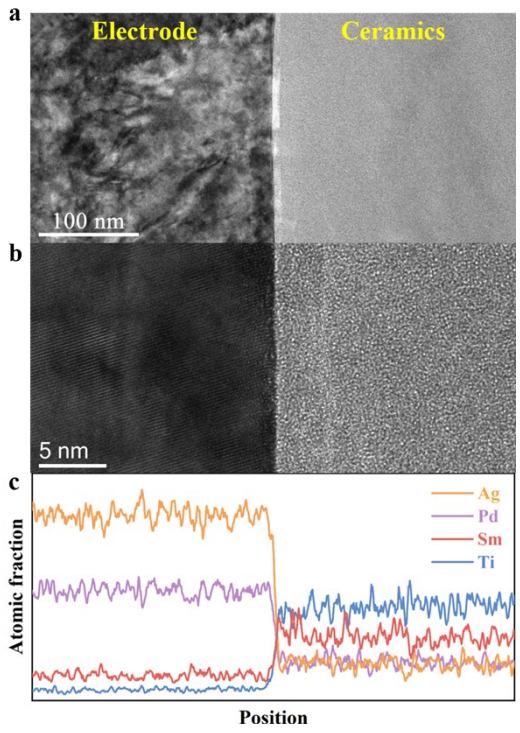

Figure S2. (a) The TEM bright-field and (b) high resolution images of dielectric-electrode interfaces of BKLNSL MLCCs, with the (c) corresponding elemental distribution.

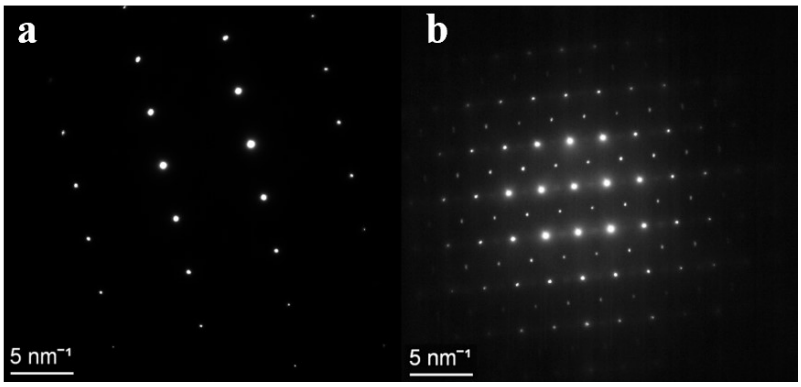

Figure S3. The selected area electron diffraction (SAED) of (a) electrode and (b) dielectric area in BKLNSL MLCCs.

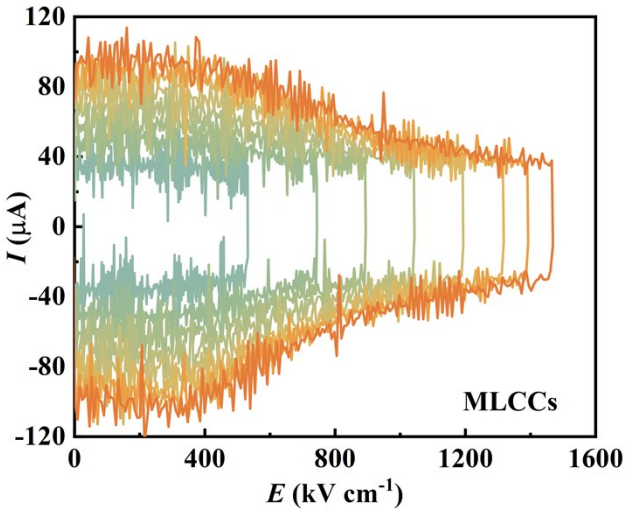

Figure S4. *I-E* loops under various electric fields of BKLNSL MLCCs.

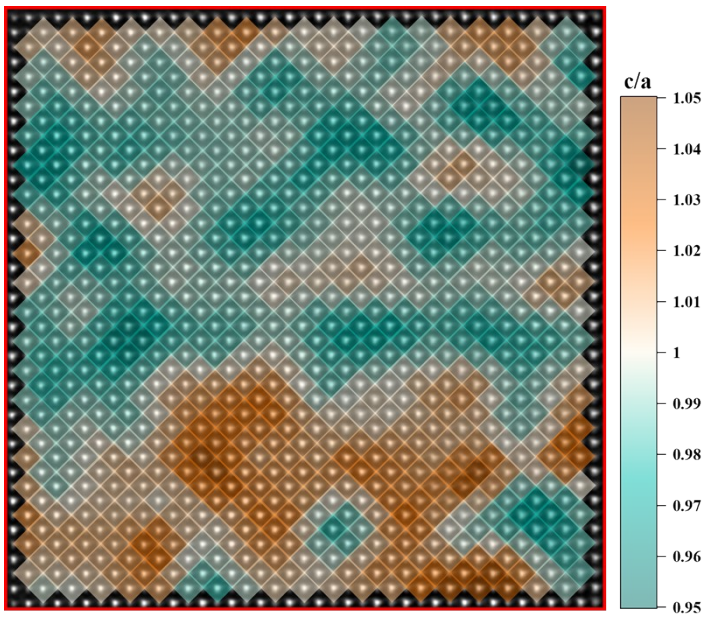

Figure S5. The represent unit cell c/a ratios of BKLNSL ceramics along $[100]_c$.

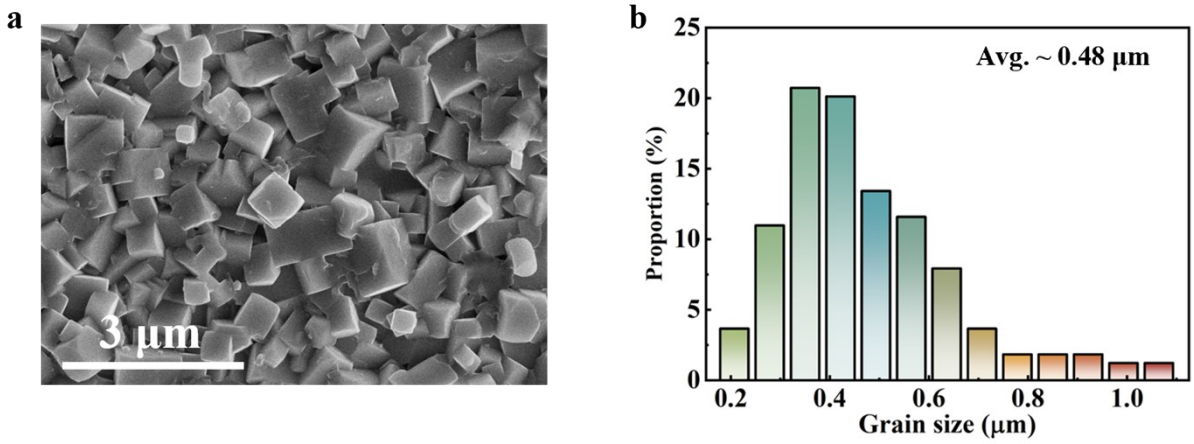

Figure S6. (a) SEM image of BKLNSL ceramics and (b) corresponding statistics of grain sizes.

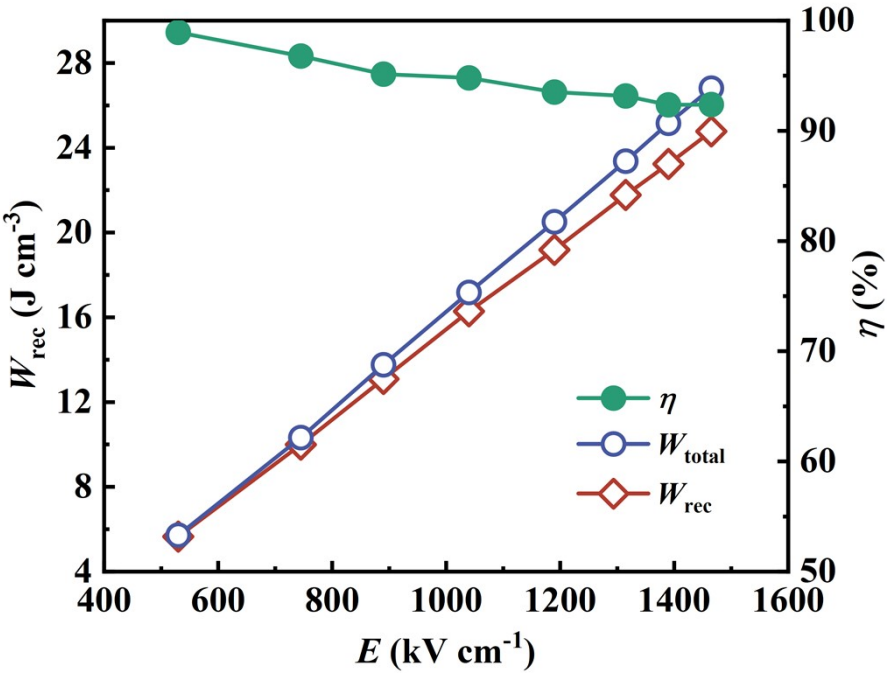

Figure S7. Evolution in ESP of BKLNSL MLCCs as a function of electric field.

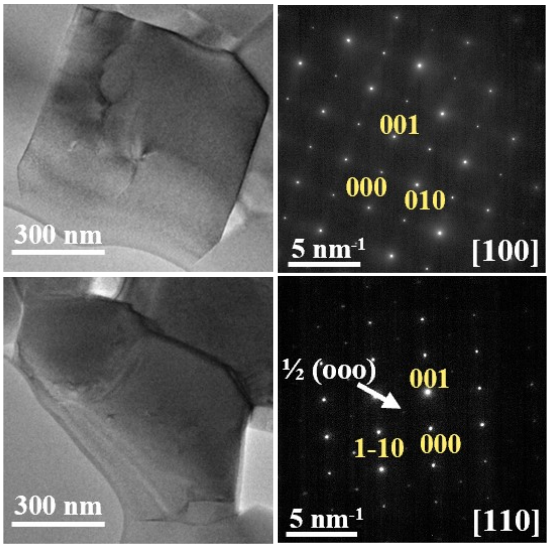

FigureS8. TEM and corresponding SAED images of BKLNSL ceramics along $[100]_c$ and $[110]_c$ axes.

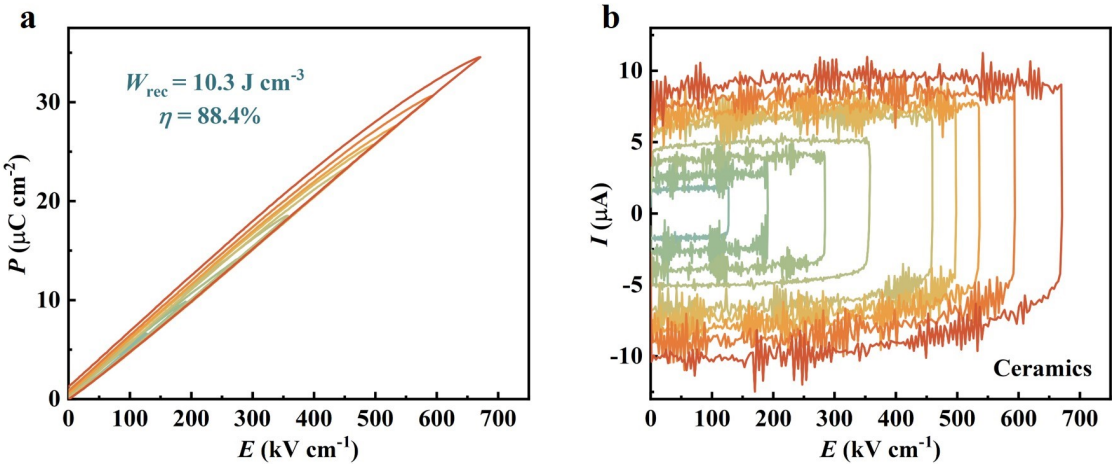

Figure S9. Evolution in (a) *P-E* loops and (b) corresponding *I-E* loops of BKLNSL bulk ceramics as a function of applied electric field.

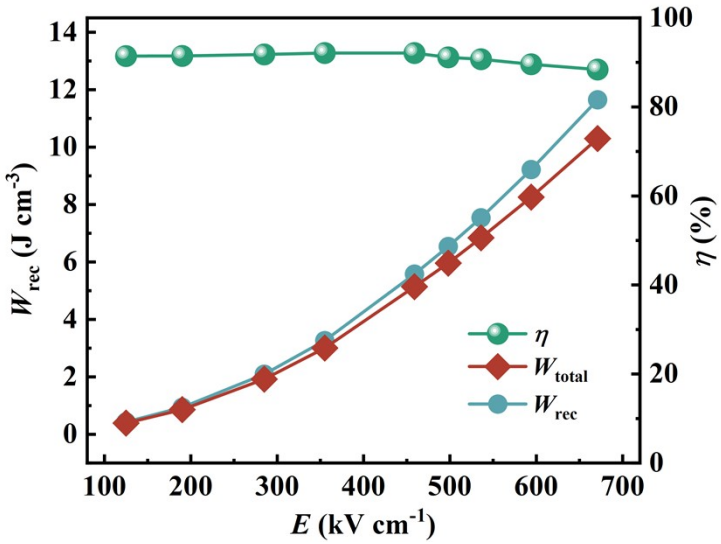

Figure S10. The ESP of BKLNSL bulk ceramics as a function of applied electric field.

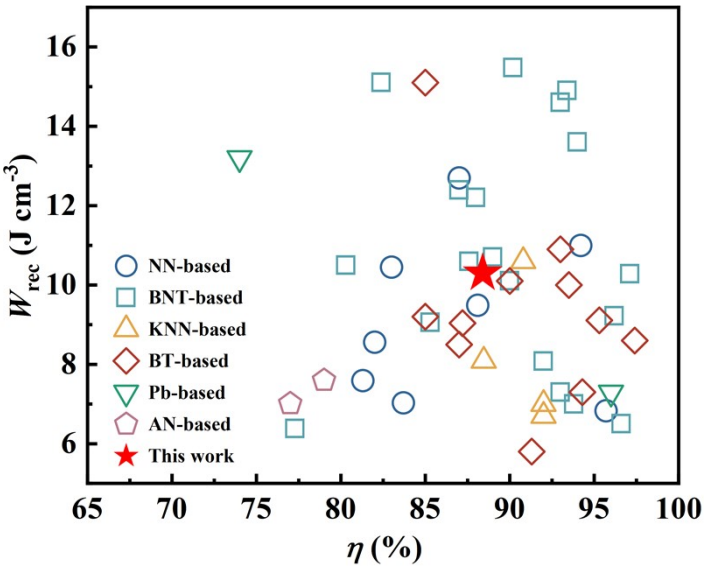

Figure S11. Comparison of W_{rec} and η of BKLNSL bulk ceramics with those of recently reported state-of-the-art RFEs.[1–46]

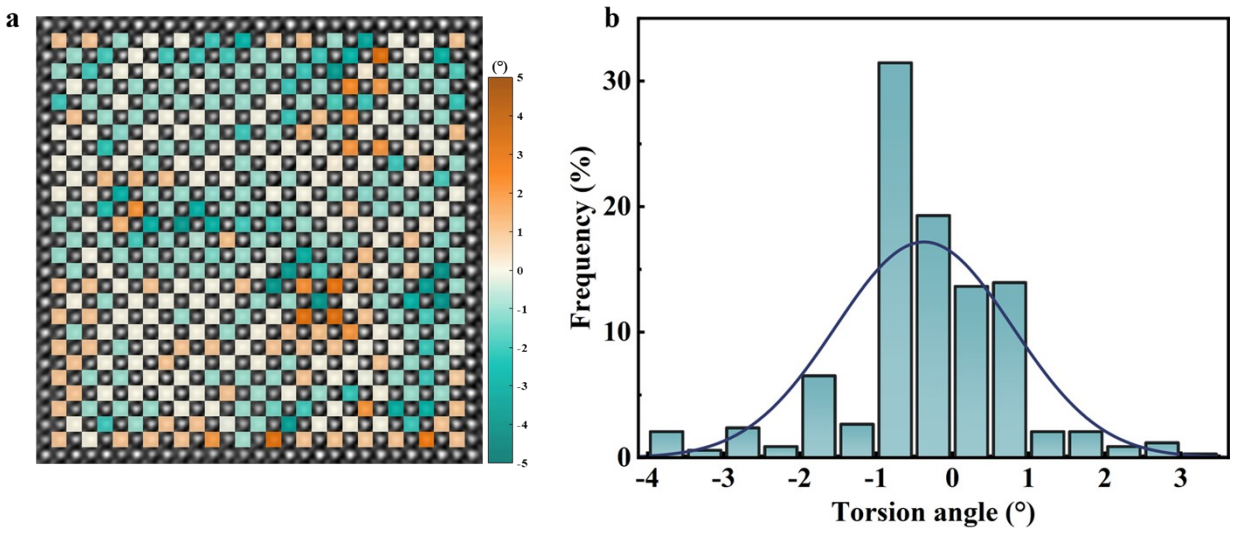

Figure S12. (a) Distribution of oxygen octahedral rotation and (b) corresponding statistics of torsion angles along the $[100]_c$ zone axis.

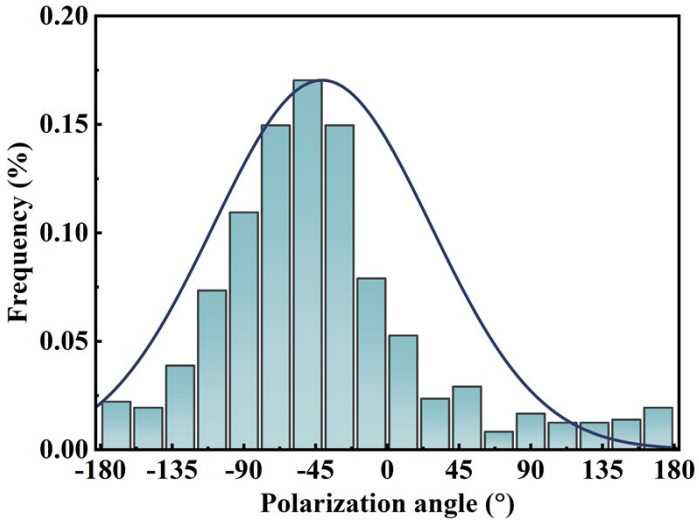

Figure S13. Statistical distribution of polarization angles along the $[100]_c$ zone axis.

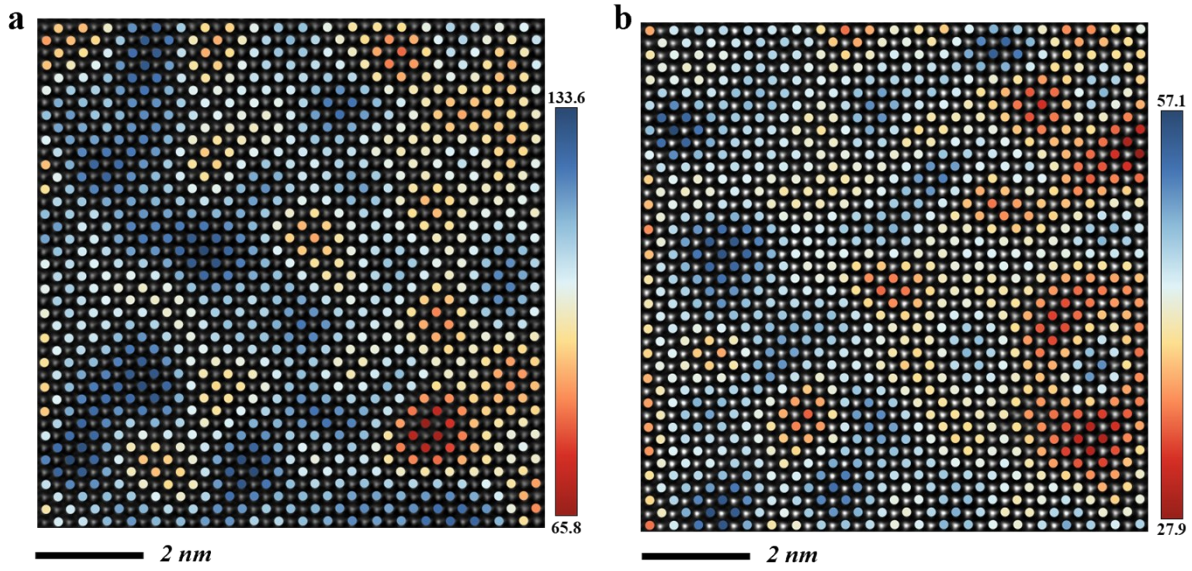

Figure S14. (a) A-site and (b) B-site atomic intensities of BKLNSL ceramics along $[100]_c$.

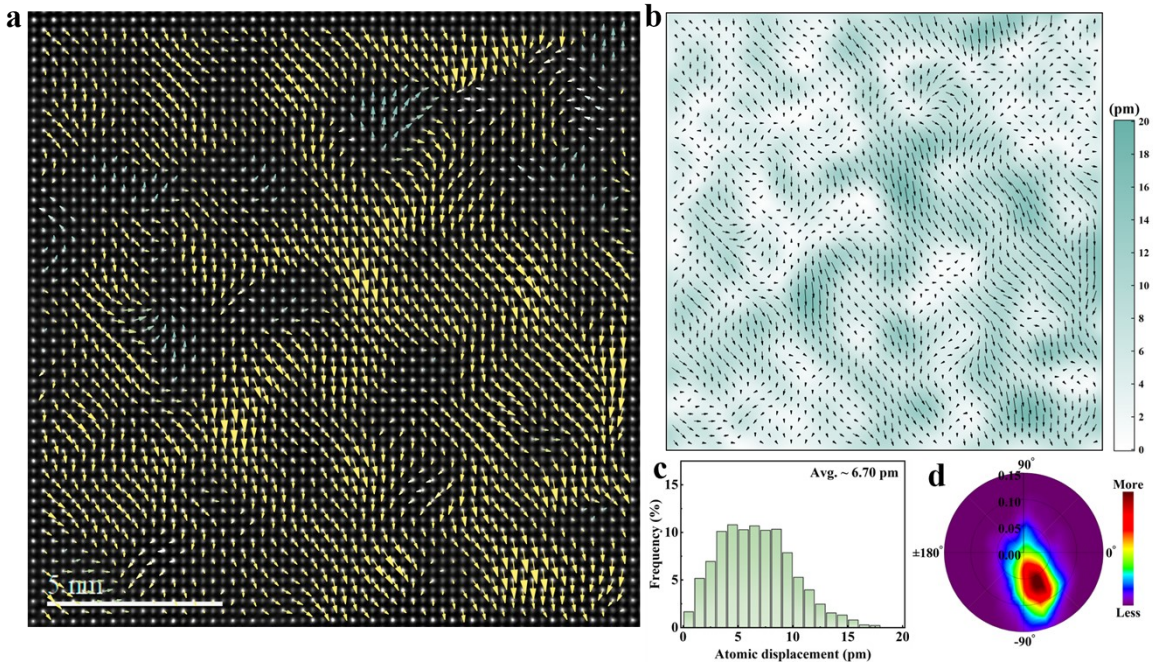

Figure S15. (a)-(b) Supplemental distribution mapping for polar displacement vectors of BKLNSL ceramics along the $[100]_c$ zone axis, along with (c)-(d) their corresponding statistical distributions.

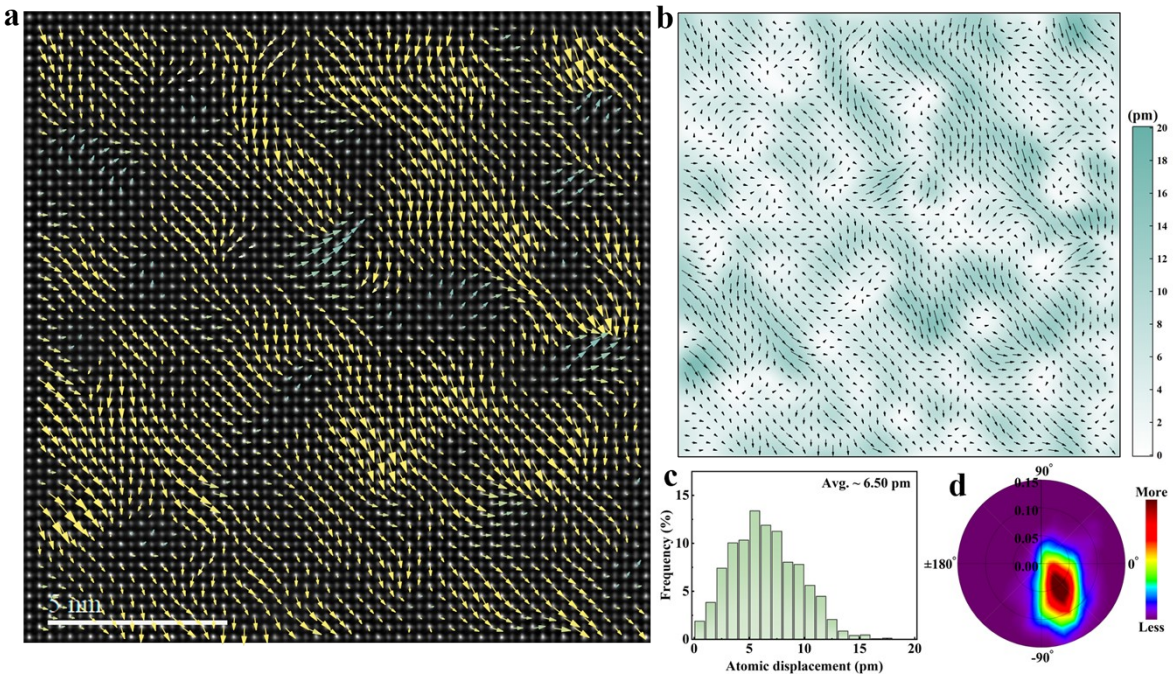

Figure S16. (a)-(b) Supplemental distribution mapping for polar displacement vectors of another region in BKLNSL ceramics along the $[100]_c$ zone axis, along with (c)-(d) their corresponding statistical distributions.

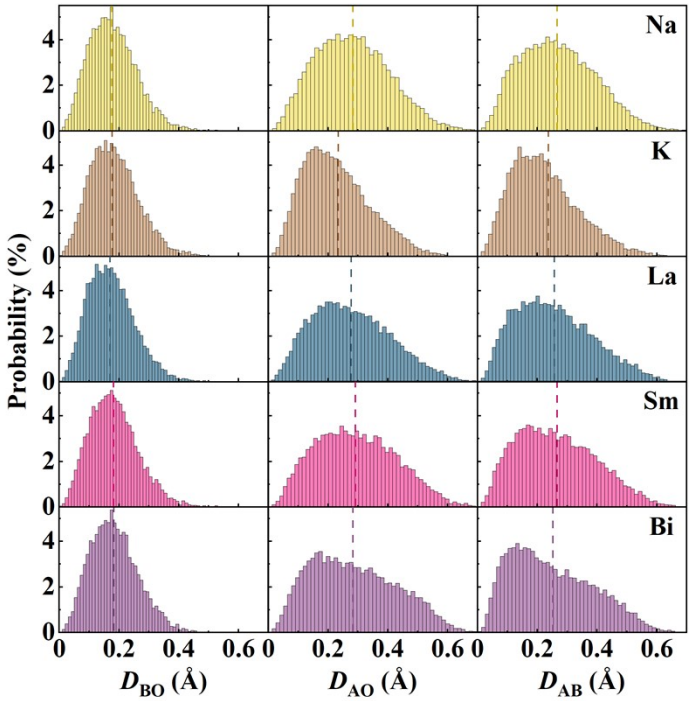

Figure S17. The statistical distributions of D_{BO} surrounding different A-site cations, D_{AO} and D_{AB} of different A-site cations, respectively and the vertical lines indicate the average values.

Table S2. Statistic values of D_{AO} and D_{AB}

Elements	$<D_{AO}>$ (Å)	σD_{AO} (Å)	$<D_{AB}>$ (Å)	σD_{AB} (Å)
Na	0.283	0.124	0.271	0.125
K	0.229	0.114	0.226	0.113
La	0.279	0.131	0.258	0.130
Sm	0.294	0.134	0.266	0.132
Bi	0.287	0.143	0.251	0.138

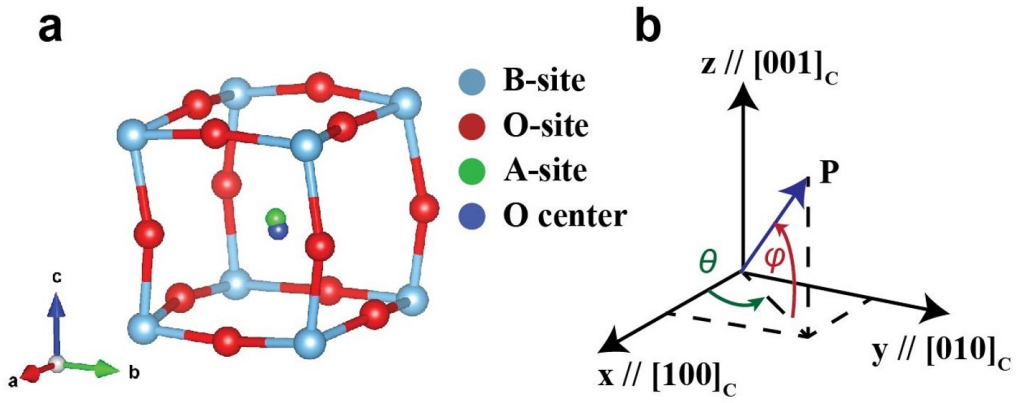

Figure S18. A schematic diagram of (a) the calculation of the polarisation within the single perovskite unit cell and (b) the polarisation vector, $\vec{P}$ defined by the azimuth angle θ and elevation angle φ relative to the pseudocubic $[100]_c$, $[010]_c$ and $[100]_c$ parent perovskite axes.

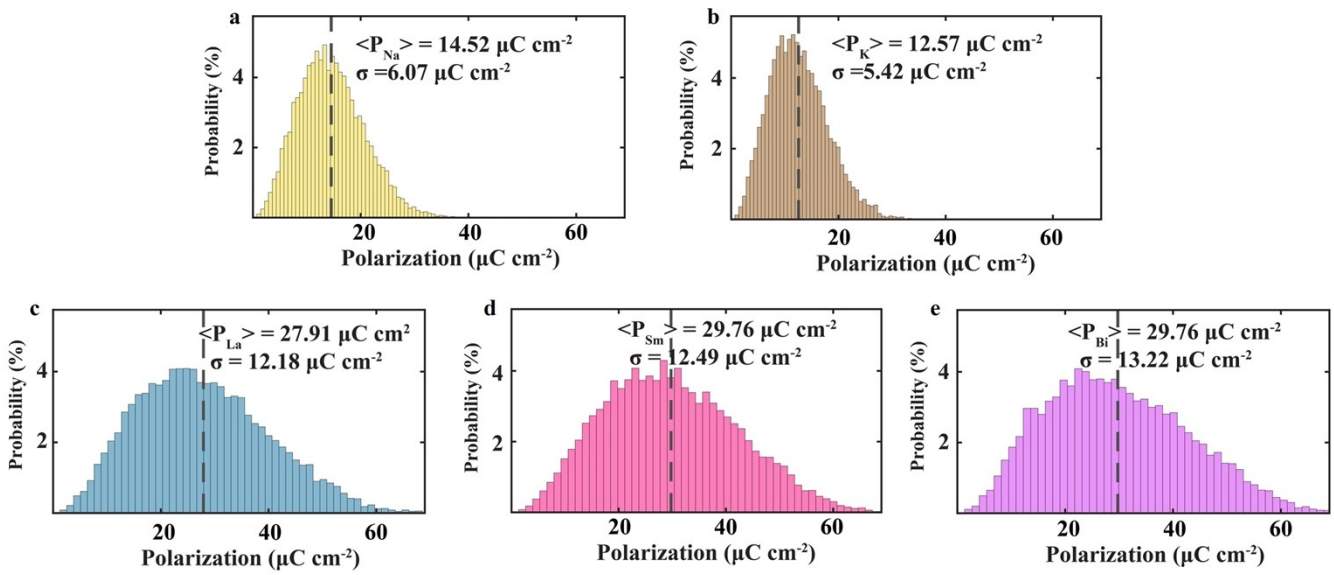

Figure S19. The statistical distributions of the magnitudes of cell polarization with (a) Na, (b) K, (c) La, (d) Sm and (e) Bi as the A-site cations, respectively and the vertical lines indicate the average values.

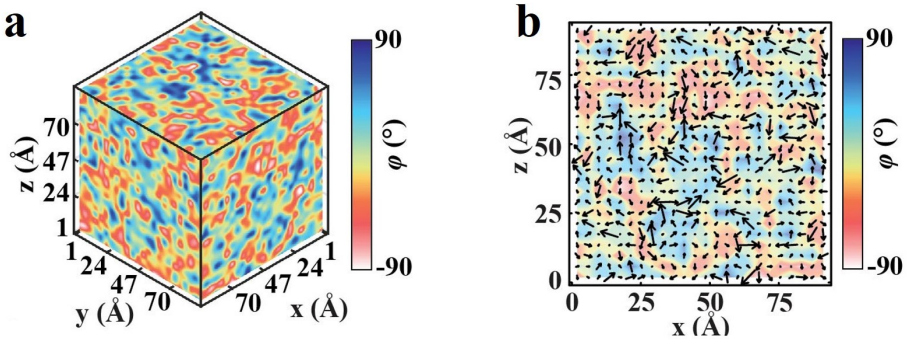

Figure S20. The (a) 3D distribution and the (d) 2D slice of the calculated elevation angles *φ*.

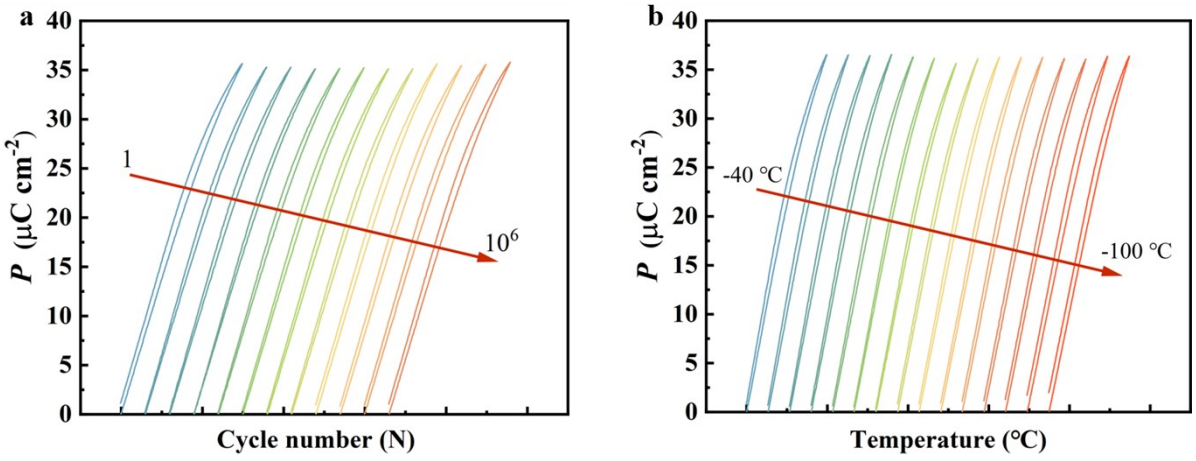

Figure S21. *P-E* loops of BKLNSL MLCCs at different (a) cycle numbers and (b) temperatures.

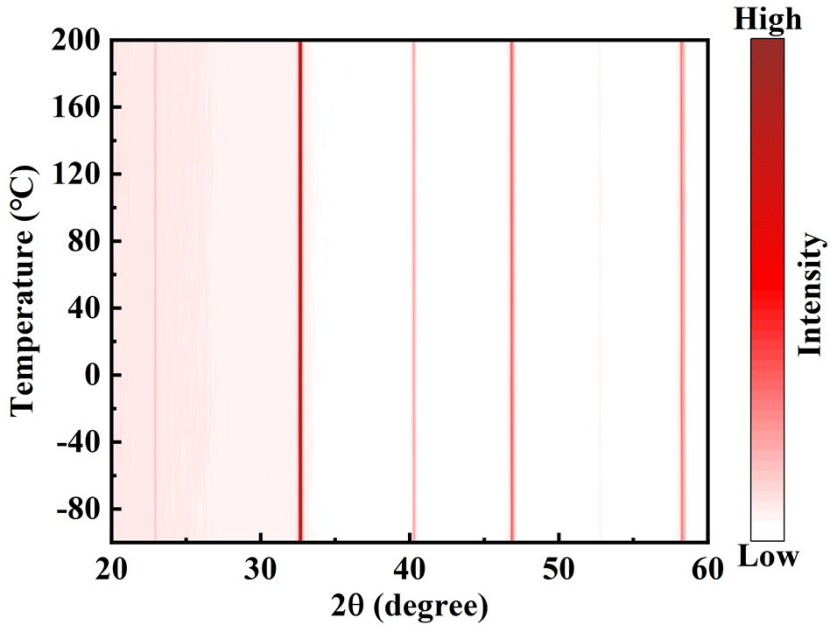

Figure S22. XRD patterns of BKLNSL ceramics under different temperatures.

Reference

1 F. Chen, M. Chen, J. Zhang, W. Liu, H. Du, Q. Zong, H. Yu, Y. Zhang, J. Hao, J. Wang, J. Zhai. *ACS Nano* **2025**, *19*, 1809–1818.

2 Z. Lv, T. Lu, Z. Liu, T. Hu, Z. Hong, S. Guo, Z. Xu, Y. Song, Y. Chen, X. Zhao, Z. Lin, D. Yu, Y. Liu, G. Wang. *Adv. Energy Mater.* **2024**, *14*, 2304291.

3 S. M. Wang, J. Qian, G. L. Ge, F. Q. Zhang, F. Yan, J. F. Lin, L. M. Tang, M. H. Yang, Z. B. Pan, X. Wei, B. Shen, Z. F. Liu, J. W. Zhai. *Adv. Energy Mater.* **2025**, *15*, 2403926.

4 W. J. Cao, R. J. Lin, X. Hou, L. Li, F. Li, D. F. Bo, B. H. Ge, D. S. Song, J. Zhang, Z. X. Cheng, C. C. Wang. *Adv. Funct. Mater.* **2023**, *33*, 2301027.

5 L. Chen, F. X. Long, H. Qi, H. Liu, S. Q. Deng, J. Chen. *Adv. Funct. Mater.* **2022**, *32*, 2110478.

6 D. Li, D. Zhou, D. Wang, W. Zhao, Y. Guo, Z. Shi. *Adv. Funct. Mater.* **2022**, *32*, 2111776.

7 F. Su, Z. Yu, Y. Zhang, H. Wang, Z. Xu, A. Tian, Z. Sui, Y. Lv, J. Fu, X. Shi, H. Qi, T. Hu, Z. Fu, R. Zuo. *Adv. Funct. Mater.* **2025**, *35*, 2500988.

8 K. B. Xi, Y. H. Li, M. P. Zheng, M. K. Zhu, Y. D. Hou. *Adv. Funct. Mater.* **2025**, e11375.

9 H. Y. Zhao, W. J. Cao, C. Liang, C. Y. Wang, C. C. Wang, Z. X. Cheng. *Adv. Funct. Mater.* **2025**, *35*, 2411954.

10 L. Chen, T. F. Hu, X. M. Shi, H. F. Yu, H. Zhang, J. Wu, Z. Q. Fu, H. Qi, J. Chen. *Adv. Mater.* **2024**, *36*, 2313285.

11 L. Chen, N. Wang, Z. F. Zhang, H. F. Yu, J. Wu, S. Q. Deng, H. Liu, H. Qi, J. Chen. *Adv. Mater.* **2022**, *34*, 2205787.

12 Y. G. Chen, Z. T. Zhu, L. F. Zhu, J. P. Xu, H. J. Luo, H. Li, W. Yin, L. J. Liu, J. Zhang, H. Liu, J. Chen. *Adv. Mater.* **2025**, *37*, 2420566.

13 D. F. Li, Z. H. Zheng, B. Yang, L. Y. Chen, D. Shi, J. M. Guo, C. W. Nan. *Adv. Mater.* **2025**, *37*, 2409639.

14 N. N. Luo, X. F. He, C. Xu, Z. G. Chen, K. Zhao, Z. Y. Cen, X. Y. Chen, D. L. Shan, Y. Y. Liu, Z. B. Liu, H. Xie, Y. Zhu, H. B. Huang, J. F. Li, S. J. Zhang. *Adv. Mater.* **2025**, *37*, 2420258.

15 L. Y. Zhang, R. Y. Jing, Y. Y. Huang, Y. L. Yang, Y. Li, M. Y. Tang, S. Y. Cao, Z. B. Chen, F. Gao, Y. X. Du, S. Y. Zhou, J. W. Zhao, S. Y. Liu, D. W. Wang, S. J. Zhang, L. Jin. *Adv. Mater.* **2024**, *36*, 2406219.

16 W. J. Cao, L. Li, K. Chen, X. C. Huang, F. Li, C. C. Wang, J. Zheng, X. Hou, Z. X. Cheng. *Adv. Sci.* **2024**, *11*, 2409113.

17 L. Chen, F. Li, B. Gao, C. Zhou, J. Wu, S. Deng, H. Liu, H. Qi, J. Chen. *Chem. Eng. J.* **2023**, *452*, 139222.

18 T. Deng, Z. Liu, T. Hu, K. Dai, Z. Hu, G. Wang. *Chem. Eng. J.* **2023**, *465*, 142992.

19 Q. Liao, T. Deng, T. Lu, Z. Liu, N. Narayanan, S. Li, S. Yan, Y. Bao, Y. Liu, G. Wang. *Chem. Eng. J.* **2024**, *488*, 150901.

20 Y. Ning, Y. Pu, Z. Chen, L. Zhang, C. Wu, X. Zhang, B. Wang, J. Zhang. *Chem. Eng. J.* **2023**, *476*, 146673.

21 Y. Pan, Q. Dong, J. Huang, X. Chen, X. Li, H. Zhou. *Chem. Eng. J.* **2024**, *497*, 154695.

22 N. Weng, J. Zhang, Z. Wang, H. Wang, L. Wang, J. Wang, Y. Wang. *Chem. Eng. J.* **2024**, *485*, 149947.

23 Y. Zhang, A. Xie, A. Tian, J. Lei, Z. Li, X. Jiang, X. Xie, X. Gao, X. Er, L. Liu, T. Li, A. Rahman, R. Zuo. *Chem. Eng. J.* **2025**, *507*, 160821.

24 M. Zhao, X. Shen, J. Wang, J. Wang, J. Zhang, L. Zhao. *Chem. Eng. J.* **2023**, *478*, 147527.

25 J. Zhou, D. Liu, R. Chen, K. Zhang, R. Jin, H. Sun, Y. Feng, X. Wei, Z. Xu, R. Xu. *Chem. Eng. J.* **2024**, *496*, 154369.

26 D. Li, D. Xu, W. Zhao, M. Avdeev, H. Jing, Y. Guo, T. Zhou, W. Liu, D. Wang, D. Zhou. *Energy Environ. Sci.* **2023**, *16*, 4511–4521.

27 T. Deng, T. Hu, Z. Liu, C. Yao, K. Dai, F. Cao, Z. Hu, G. Wang. *Energy Storage Materials* **2024**, *71*, 103659.

28 S. Li, T. Hu, H. Nie, Z. Fu, C. Xu, F. Xu, G. Wang, X. Dong. *Energy Storage Materials* **2021**, *34*, 417–426.

29 Z. Lv, B. Han, Z. Liu, S. Guo, K. Dai, F. Cao, Z. Hu, G. Wang. *Energy Storage Materials* **2025**, *77*, 104205.

30 M. Zhang, H. Yang, Y. Lin, Q. Yuan, H. Du. *Energy Storage Materials* **2022**, *45*, 861–868.

31 Z. Xu, Z. Liu, K. Dai, T. Lu, Z. Lv, Z. Hu, Y. Liu, G. Wang. *J. Mater. Chem. A* **2022**, *10*, 13907–13916.

32 H. Liu, Z. Sun, J. Zhang, H. Luo, Q. Zhang, Y. Yao, S. Deng, H. Qi, J. Liu, L. C. Gallington, J. C. Neuefeind, J. Chen. *J. Am. Chem. Soc.* **2023**, *145*, 11764–11772.

33 Z. Sun, J. Zhang, H. Luo, Y. Yao, N. Wang, L. Chen, T. Li, C. Hu, H. Qi, S. Deng, L. C. Gallington, Y. Zhang, J. C. Neuefeind, H. Liu, J. Chen. *J. Am. Chem. Soc.* **2023**, *145*, 6194–6202.

34 M. Liu, C. Ming, Z. Liu, H. Liu, B. Han, N. Narayanan, X. Liu, K. Dai, T. Lu, X. Chen, Z. Hu, Y. Liu, G. Wang. *Mater. Horiz.* **2025**, *12*, 3939–3948.

35 H. Qi, W. Li, L. Wang, L. Chen, H. Liu, S. Deng, J. Chen. *Materials Today* **2022**, *60*, 91–97.

36 J. Guo, H. Yu, Y. Ren, H. Qi, X. Yang, Y. Deng, S.-T. Zhang, J. Chen. *Nano Energy* **2023**, *112*, 108458.

37 R. Kang, Z. Wang, M. Wu, S. Cheng, S. Mi, Y. Hu, L. Zhang, D. Wang, X. Lou. *Nano Energy* **2023**, *112*, 108477.

38 C. Long, Z. Su, A. Xu, H. Huang, L. Liu, L. Gu, W. Ren, H. Wu, X. Ding. *Nano Energy* **2024**, *124*, 109493.

39 W. Shi, L. Zhang, R. Jing, Y. Huang, F. Chen, V. Shur, X. Wei, G. Liu, H. Du, L. Jin. *Nano-Micro Lett.* **2024**, *16*, 91.

40 Q. Chai, Z. Liu, Z. Deng, Z. Peng, X. Chao, J. Lu, H. Huang, S. Zhang, Z. Yang. *Nat Commun* **2025**, *16*, 1633.

41 L. Chen, S. Deng, H. Liu, J. Wu, H. Qi, J. Chen. *Nat Commun* **2022**, *13*, 3089.

42 X. Kong, L. Yang, F. Meng, T. Zhang, H. Zhang, Y.-H. Lin, H. Huang, S. Zhang, J. Guo, C.-W. Nan. *Nat Commun* **2025**, *16*, 885.

43 D. Li, Z. Liu, W. Zhao, Y. Guo, Z. Wang, D. Xu, H. Huang, L.-X. Pang, T. Zhou, W.-F. Liu, D. Zhou. *Nat Commun* **2025**, *16*, 188.

44 Z. Wang, D. Li, W. Liu, L. He, D. Xu, J. Liu, J. Ren, X. Wang, Y. Liu, G. He, J. Bao, Z. Fang, G. Yan, X. Liang, T. Zhou, W. Zhao, W. Liu, D. Wang, D. Zhou. *Nat Commun* **2025**, *16*, 2892.

45 H. Yu, T. Hu, H. Wang, H. Qi, J. Wu, R. Zhang, W. Fang, X. Shi, Z. Fu, L. Chen, J. Chen. *Nat Commun* **2025**, *16*, 886.

46 W. Zhao, D. Xu, D. Li, M. Avdeev, H. Jing, M. Xu, Y. Guo, D. Shi, T. Zhou, W. Liu, D. Wang, D. Zhou. *Nat Commun* **2023**, *14*, 5725.